

Development of a computational tool for a new fluorescence microscopy technique

Author: Sara Lumbreras Navarro

Facultat de Física, Universitat de Barcelona, Diagonal 645, 08028 Barcelona, Spain.

Advisor: Mario Montes Usategui

Abstract: Trustworthy simulations of microscopy images are hard to find. This research aims to develop an image software simulator of confocal microscopes focusing on the Superfast Confocal Microscopy through Enhanced Acousto-Optic Modulation (SCREAM). The simulation code is written in Python, is based on physical principles and it computes the image produced by the microscope using different filtering methods. The code was used to study cross-talk, XY resolution and some results not previously described in the literature.

I. INTRODUCTION

Nowadays the confocal microscope is the king in the field of fluorescence microscopy due to its contrast, resolution, and sectioning capability, allowing 3D sample reconstruction [1]. The imaging of fluorescent samples present out-of-focus light resulting in a degradation of the final image, an obstacle to reach the resolution imposed by diffraction. Traditional confocal laser scanning microscopes (CLSM) use a single highly focused beam to scan the sample. They also use a physical pinhole to suppress the out-of-focus light. The slow speed and the high amount of light dose used makes this technology most suitable for fixed or dead samples.

Alternatively, the multiple-point approach is specially designed to overcome both, the speed and phototoxicity present on most CLSMs, being compatible with living samples. The most established implementation is the spinning disk which uses two rotatory disks at high speed reaching hundreds of frames per second. Although, they require more powerful excitation lasers and have less confocality due to cross-talk between pinholes [2]. Mechanical components introduce unwanted vibrations which could affect sensitive equipment connected to the microscope [3].

Recently, the BiOPT group has developed an innovative confocal technique called Superfast Confocal Microscopy through Enhanced Acousto-Optic Modulation (SCREAM). Combining two orthogonal Acousto-optical deflectors (AODs) and digital holography, the SCREAM can generate different excitation patterns and scanning protocols. Its versatility combines both advantages of the single and multi-point scanning methods and gets rid of the main disadvantages.

The aim of this work is to simulate the behavior of the SCREAM microscope for a better understanding of the device, comparing the XY resolution and crosstalk for the different modes that it offers.

II. SIMULATION PROGRAM ARCHITECTURE

The developed simulation is based on the physical principles of image formation and beam propagation in a reg-

ular optical setup. The program can be used to simulate the output image using different filtering methods and excitation patterns available in the SCREAM instrument. Due to our interest, it is mainly focused on grid type excitation although it can also operate with other patterns such as single-point scanning or line scanning.

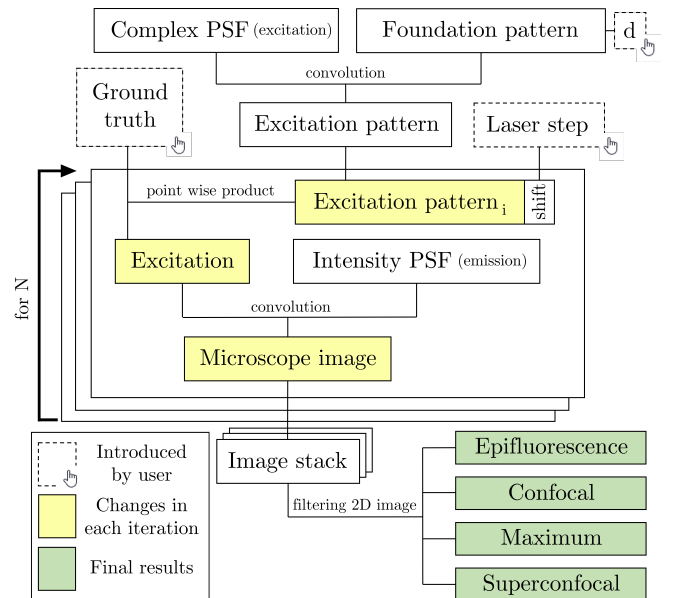


FIG. 1: Flow chart of the simulation program.

A. Excitation pattern

To model the excitation pattern the complex 3D Point Spread Function (complex PSF) of the system and the foundation pattern ($f_0(x, y)$) are used.

The foundation pattern is a 2D binary array where the laser positions take the value of 1. For the grid type excitation, d is the distance between two consecutive laser spot positions and defines the periodicity. It is a parameter chosen by the user in physical units.

The PSF is the response of an optical system to the stimulation of a point light source. Let $\hat{h}(x, y, z)$ be the complex PSF of our system where $z = 0$ corresponds to the focal plane. The equation that describes it is the

diffraction integral of a circular opening (equation 1) [4].

$$\hat{h}(x, y, z) = C \int_0^1 J_0 \left[\frac{kNA}{n_i} (x^2 + y^2)^{\frac{1}{2}} \rho \right] e^{\frac{ikz}{2} \frac{\rho NA^2}{n_i^2}} \rho d\rho \quad (1)$$

This approximation is good enough considering our microscope properties ($NA = 1.2$, $\lambda = 532$ nm, $n_i = 1.33$) [2]. For more accurate PSF might be computed using vectorial theory [5].

The convolution between the complex PSF and the foundation pattern is the desired excitation pattern ($f(x, y, z)$) where the normalized intensity is taken (equation 2). Figure 2 schematizes the operation.

$$f(x, y, z) = |\hat{h}(x, y, z) * f_0(x, y)|^2 \quad (2)$$

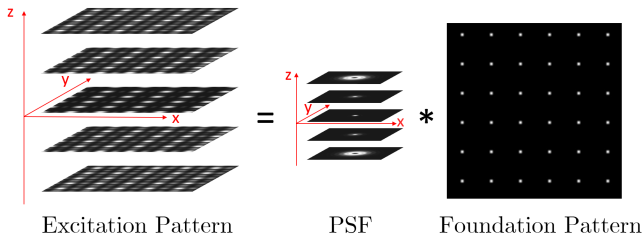


FIG. 2: Scheme of the operation computed with the PSF and the foundation pattern to obtain the excitation pattern.

On a real optical setup the multiple foci excitation can be obtained either using a microlens array or digital holography. The SCREAM microscope uses holograms calculated with the Gerchberg-Saxton algorithm to maximize efficiency [6]. The generally pseudo-random phase resulting from the algorithm is also taken into account on the foundation pattern.

Figure 3 shows the light distribution along the z axis for different methods. If we generate the multi-point excitation pattern with a lens array, we will obtain replicas of the pattern in different planes and positions due to the Talbot effect which highly depends on the periodicity. For higher densities, replicas are closer whereas for lower the behavior is the opposite.

The resulting pattern from the Gerchberg-Saxton is uncertain and replicas are not clearly formed on the out-of-focus planes. The algorithm also breaks the axial symmetry and tends to spread the light intensity, avoiding excitation of other planes. Besides, the acoustic wave propagation inside the AOD crystal introduce a shift of the hologram which we are not taking into account in this simulation for simplicity. For that reason, the micro lens array approach is the one considered.

B. Ground truth

We manually define the ground truth as a 3D grayscale image that simulates the fluorophore arrangement on a

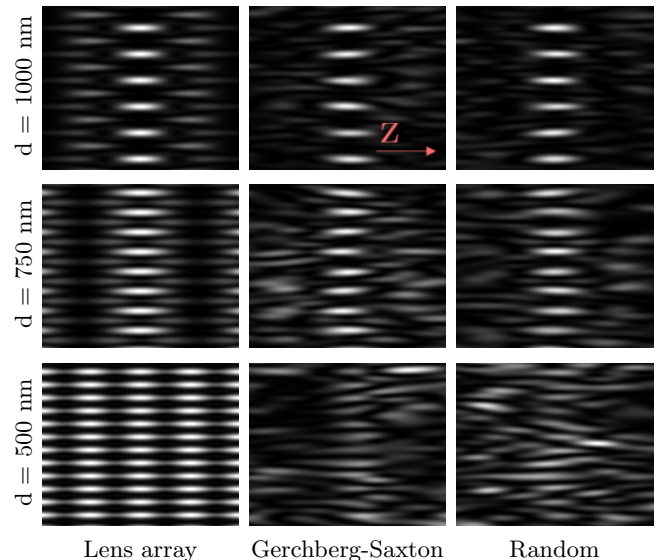


FIG. 3: Excitation pattern ZY cut for different periodicities and methods. The corresponding phase is added to the foundation pattern for each method.

real sample. Ground truth images for this study are specially designed to suit the experiment purpose and consist of binary images with target fluorophores. The ground truth is denoted as $GT(x, y, z)$ in what follows.

C. Microscope image formation

The SCREAM uses a scanning method in which the excitation pattern is shifted and an image of the fluorescent emission is obtained. The program repeats this scheme until the whole field of view is covered.

• Pattern shift

The grid excitation pattern is shifted from left to right for each row, then returned to the original position and shifted down, repeating this procedure until the whole sample is uniformly illuminated. The distance shifted is defined by the laser step, a parameter chosen by the user in physical units. The total amount of shifts needed, N , is defined by both the laser step and the periodicity. From now on $f_i(x, y, z)$ is a shifted excitation pattern.

• Excitation

To simulate the excitation phenomena it is assumed that fluorophores behave linearly, the emission is proportional to the excitation. Given one excitation pattern shift, the pointwise product with the ground truth represents the excited ground truth and reflects the level at which each fluorophore is emitting.

$$GT_{ex_i}(x, y, z) = GT(x, y, z) \cdot f_i(x, y, z) \quad (3)$$

- Microscope imaging

The theory of image formation for an optical setup establishes that the formed image is the convolution between the object and the intensity PSF of the system plus an additive term of noise [7]. Assuming that the light emitted by the fluorophores is incoherent, the light intensity coming from different fluorophores should be added. The same PSF will be used to model the emission and the excitation, a frequent approximation used in the microscopy field (zero Stokes shift).

$$Im_i(x, y) = \sum_k^{\#planes} (GT_{ex_i}(x, y, z_k) * |\hat{h}(x, y, z_k)|^2) + n(x, y). \quad (4)$$

For each shift, a microscope image is taken creating an image stack after the N iterations saved for future processing.

D. Filtering algorithms

To obtain the final 2D image the program processes the image stack using different filtering algorithms.

- Epifluorescence

The epifluorescence microscope technique uniformly illuminates the whole sample at the same time. To obtain an approximation of an image obtained with this technique using the stack, all the frames are averaged (equation 5).

$$Epi(x, y) = \frac{\sum_{i=1}^N Im_i(x, y)}{N} \equiv Av(x, y) \quad (5)$$

- Confocal

The program also creates a pinhole array centered with the beam grid for each shift reproducing the operation of a multi-point confocal. In a regular confocal microscope the pinhole size is set at 1 Airy unit (≈ 200 nm) for optimal filtering. Smaller pinholes improve resolution but it compromises the signal to noise ratio (SNR) [8].

The simulation runs grid pattern excitation which could be a first approximation of the spinning disk. Regarding sectioning capability, it is found that beam density and pinhole size are the parameters that have the greatest impact on the final result.

$$Conf(x, y) = \sum_i^N Im_i(x, y) \cdot \text{pinhole}_i(x, y) \quad (6)$$

- Maximum

Computing the maximum value for each pixel of the stack is a simple operation that has good results in terms of resolution and sectioning capability [9]. This operation is fast and easy to implement.

$$\text{Max}(x, y) = \text{Max}_{i=1 \rightarrow N} (Im_i(x, y)) \quad (7)$$

- Superconfocal

Looklike confocal images can be obtained by an algorithm which consists of computing the operation described in equation 8 [9]. It has good sectioning capabilities similar to a real confocal microscope. γ has to be chosen properly depending on the SNR, on the laboratory conditions $\gamma = 2$ has proved to give an optimal result.

$$\text{Superconf}(x, y) = \text{Max}(x, y) + \text{Min}(x, y) - \gamma Av(x, y) \quad (8)$$

E. Z scan

Sectioning capability of confocal microscopes allows 3D reconstruction of samples. This feature is also added to the simulation program by simply shifting the ground truth up and down, simulating the focus change in a real microscope.

III. RESULTS

Once we were sure that the developed program was satisfactorily simulating the real microscope, the next step was to study the resolution in XY and cross-talk along the Z axis. The study focuses on comparing the results varying different parameters relevant the corresponding experiments. We will use the lens array excitation pattern for the following experiments for the reason previously mentioned.

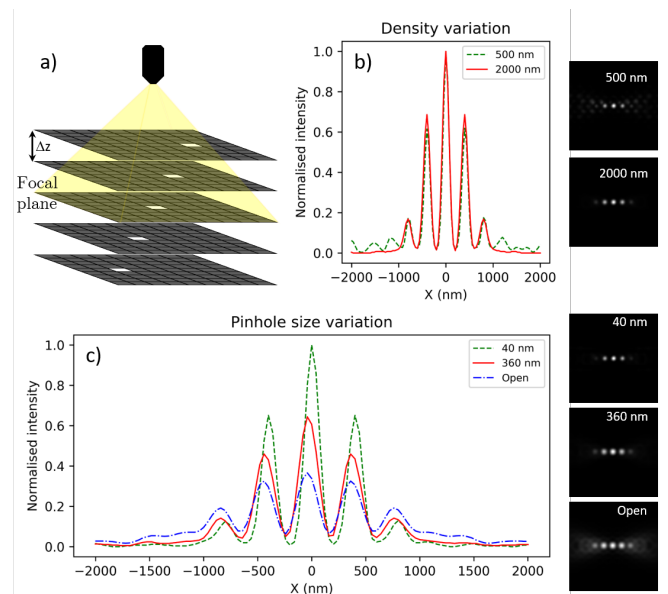


FIG. 4: a) Shows a scheme of the ground truth used for the study, a set of fluorescent spots uniformly separated along the X and Z directions. b) and c) Plots show intensity profiles for the central row using the confocal filtering method. b) Shows the results when varying the periodicity for the same pinhole size of 120 nm. c) Shows variations on the pinhole size for a periodicity $d = 1000$ nm. The 2D images are displayed on the right of each plot.

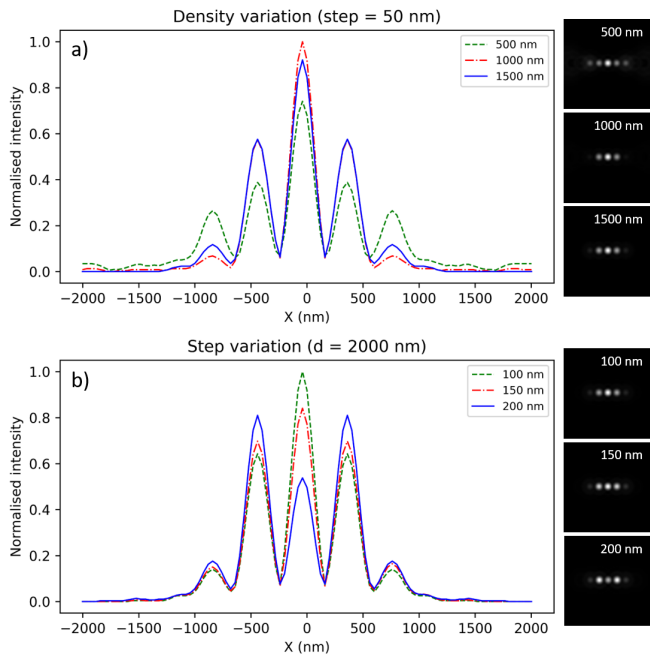


FIG. 5: Intensity profiles for the central row using the superconfocal filtering method. a) Shows the results when varying the excitation periodicity for a laser step = 50 nm. b) Shows the difference when varying the laser step for a density of $d = 2000$ nm. The result images are shown on the right for each plot.

- Cross-talk

The ground truth designed for this study is a 3D stack with 11 planes separated $\Delta z = 250$ nm. The spots are shifted in the X direction by 500 nm, see figure 3 a) for a scheme of the ground truth.

A first study was performed on the confocal filtering method varying the parameters that could affect cross-talk. As we see in the intensity profile in figure 4 c), the image contrast is significantly enhanced when reducing the pinhole size, which leads to a better sectioning capability. An open pinhole replicates the epifluorescent result where the out-of-focus light is clearly visible. Figure 4 b) shows that low vs high densities only affect the excitation of deeper planes. Images obtained with high-density excitation patterns exhibits artifacts due to the replicas in other planes that are not present for lower densities.

A similar study tested the superconfocal algorithm, the one that the SCREAM microscope most frequently because it offers the best visual results and is easy to implement on the camera software. This study focuses on varying excitation periodicity and the laser step. Using the same ground truth described before the results in figure 5 a) show that for this method, even high densities achieve a good sectioning capability. Surprisingly, $d = 1000$ nm achieves slight better results than $d = 1500$ nm which might be due to the replicas. It is also interesting how for higher laser steps the ground truth is not well sampled, which is the case in figure 5 b) for laser step = 200 nm where the central fluorophore is not illuminated enough.

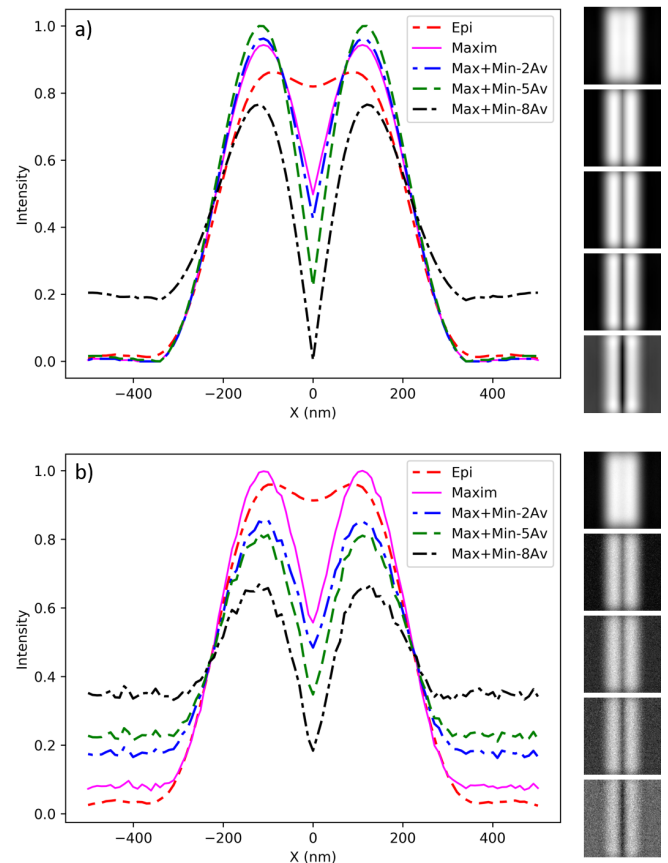


FIG. 6: Intensity profiles for different methods of two parallel lines as ground truth. a) Noiseless, b) Gaussian noise added. See on the right the image results in the same order as in the plot legend.

- XY resolution

The ground truth designed to study the XY resolution on a single plane is a 2D binary image with two parallel lines separated 220 nm. This distance is close to the resolution limit described by diffraction theory. We will be comparing the results obtained with epifluorescence, the maximum, and superconfocal for different γ values. Figure 6 a) shows an unexpected gain on resolution for higher γ values. However, there is a top γ value at which the average term of the equation is dominant and the resulting image exhibits amplification of the background.

For more realistic results, Gaussian noise with a standard deviation of 10% of the maximum value is added. It is found that for higher γ the two lines are better resolved, although it means a drop in SNR, as can be seen in figure 6 b).

- 3D reconstruction

Using the Z scan feature we made 3D reconstruction for the different filtering methods. First, we designed a 3D spherical surface of $4.5 \mu\text{m}$ radius as ground truth to see if the shape was recovered after imaging. Figure 7 shows that epifluorescence hardly recovers the spherical

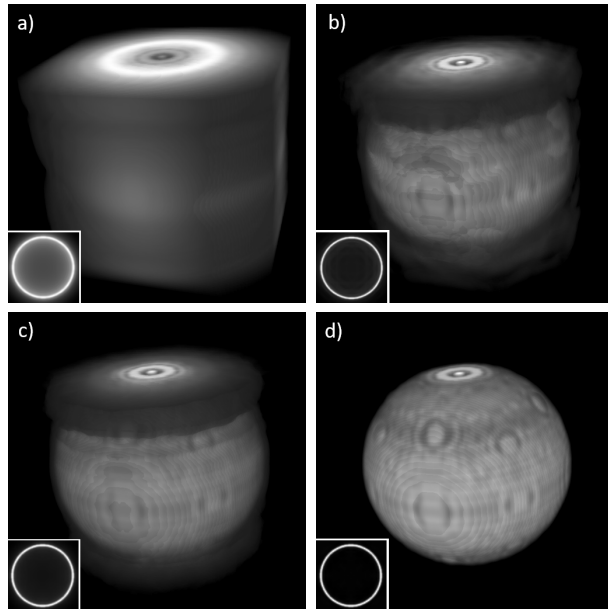


FIG. 7: 3D reconstruction of a spherical surface using the Z scan method. a) Epifluorescence, b) Maximum, c) Confocal, d) Superconfocal. Insets show the XY section of the corresponding method.

shape whereas the superconfocal almost perfectly reproduces it. Some artifacts can be seen on the surface which were also in the ground truth as a result of computing discretization.

Another result used a real biological image of mitochondria taken with an electron microscope as ground truth [10]. The sample is $3.84 \times 3.84 \times 0.825 \mu\text{m}$ and the 3D reconstruction took 4 days of computing time. Figure 8 shows the reconstructed superconfocal 3D image that presents less improvement over the epifluorescence as for such thin samples the out-of-focus light is less than the for the sphere.

IV. CONCLUSIONS

This confocal simulator approach has proved to obtain reliable results. It has helped to understand some behaviors first noticed on the real device. The impact that laser step and beam density have on the final image is of great importance. Higher densities and larger laser steps drastically reduce the number of shifts needed to cover

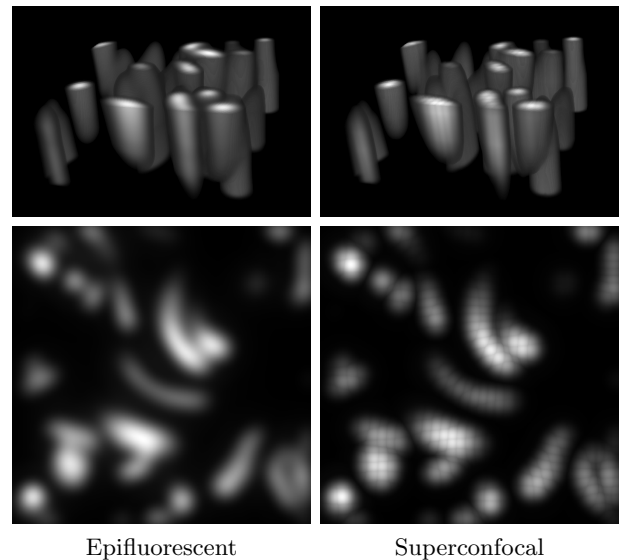


FIG. 8: Top 3D reconstruction of mitochondria using the Z scan method. Bottom pictures of an XY section.

the sample resulting in an increase of the frame rate but, reducing the image quality. The user is compromised when selecting those parameters depending on his needs or the sample properties, such as thickness. The results have also proved that the superconfocal method is a valid algorithm to compute confocal images obtaining an even better performance in 3D reconstruction.

Moreover, the images generated by the simulator could be used in a future project as massive data to train a neural network that would implement intelligent control over the laser illumination. A future improvement on the simulation could incorporate the AOD acoustic wave propagation, which will lead to a better approximation of the excitation pattern on the SCREAM device.

Acknowledgments

I would like to thank my advisor Mario Montes for his guidance during these months and Raúl Bola for his experimental feedback on the simulation results.

-
- [1] W. Amos and J. White, *Biol. Cell* **95**, 335 (2003).
 [2] J. Pawley, *Handbook of Biological Confocal Microscopy* (Springer US, 2006), 3rd ed.
 [3] A. Miranda et al., *Rev. Sci. Instrum.* **86**, 093705 (2015).
 [4] M. Born and E. Wolf, *Principles of Optics* (Cambridge University Press, 1999), 7th ed.
 [5] L. Novotny and B. Hecht, *Principles of Nano-Optics* (Cambridge University Press, 2012), 2nd ed.
 [6] R. W. Gerchberg and W. O. Saxton, *Optik* **35**, 237

- (1972).
 [7] R. Gonzalez and R. Woods, *Digital Image Processing* (2008), 3rd ed.
 [8] T. Wilson, *J. Microsc.* **244**, 113 (2011).
 [9] R. Heintzmann and P. A. Benedetti, *Appl. Opt.* **45**, 5037 (2006).
 [10] C. Xiao et al., *Front Neuroanat* **12**, 92 (2018).